Qatar Univ. Sci. J. (1997), 17(2): 431-454

PAN-AFRICAN MAGMATISM IN THE ZABARA DISTRICT, CENTRAL EASTERN DESERT, EGYPT: GEOCHEMISTRY AND PETROGENESIS

By

MOHAMED M. EL SAYED

Geology Department, Faculty of Science, Alexandria University, Egypt

النشاط المجماتي البان افريقي في منطقة زبارا وسط الصحراء الشرقية، مصر : جيوكيمياء والاصل

محمد محمد السيد

قسم الجيولوجيا / كلية العلوم / جامعة الاسكندرية / مصر

تتكون منطقة زبارا من تتابع افيوليتي وتتابع غير افيوليتي، التتابع الافوليتي يتكون من الجابرو المتحول والبازلت المتحول والمصاحبة للرسوبيات المتحولة، اما التتابع الغير افيوليتي فيتكون من البركانيات المتحولة المتوسطة والحامضية مع الجرانيت الحديث.

الرسوبيات المتحولة والحامضية التركيب تتميز بقلة عناصر الكروميوم والنيكل ولها خواص جيوكيميائية مشابهة لرسوبيات اقواس الجزر المحيطية، المتاجابرو والمتابازلت الافيوليتي له خواص ثوليتية ومشابهة من الناحية الجيوكيميائية لصخور حيد وسط المحيط الهادي، والصخور الافيوليتية تكونت بواسطة الذوبان الجزئي لمعادن الاوليفين والكلينوبيروكسين والبلاجيوكلار.

والتتابع الغير افيوليتي له خواص كلس ـ قلوية وتمثل سلسلة من تتابع التبلور الجزئي وصخور الجرانيت الحديث التي تكونت بعد التجبل والتي لها خواص قلوية تكونت بواسطة ٧٠٪ تبلور جزئي لمعادن البلاجيوكلاز، الفلسبار القلوي، البيوتيت، التيتانيت والزركون من سائل الداسيت.

Key words: *e*gypt. Ophiolite. Geochemistry. Partial melting. Fractional crystallization.

ABSTRACT

The rocks of the Zabara district include ophiolitic and non-ophiolitic sequences. The ophiolitic ones are metagabbro and metabasalt associated with metasediments, whereas the non -ophiolitic sequence includes intermediate to acidic metavolcanics and two -mica younger granites. The metasediments are felsic with SiO2 ranging from 68 to 72 wt% with relatively low Cr and Ni contents (51 ppm and 16 ppm, respectively), which suggest that felsic rocks were predominated in their source area. The Zabara metasediments are characterised by slightly flat REE patterns and have geochemical features similar to those of the ocean island arc metasediments.

The ophiolitic metagabbro and metabasalt are similar in their major and trace element contents and show a tholeiitic affinity. The ophiolitic sequence exhibits geochemical characteristics on N-MORB with very low levels of K2O, Nb, Zr, Rb and Ba and flat REE patterns. The REE modelling reveals that the ophiolitic sequence could be derived by non-modal batch partial melting of spinel lherzolite source followed by subsequent fractional crystallization of olivine, clinopyroxene and plagioclase.

The non-ophiolitic metavolcanics cover the entire spectrum from medium-K meta-andesite to high-K metadacite with calc-alkaline affinity. The metavolcanics have slightly fractionated LREE and unfractionated, flat HREE. The non-ophiolitic metavolcanics represent cogenetic fractionated sequence.

The highly evolved post-orogenic alkaline two mica granite exhibits peraluminous character and shows close similarity with the metarhyolite with repeat to major and trace elements. The granite could be modelled by about 70% fractional crystallisation of plagioclase, alkali feldpar, biotite, titanite and zircon from the dacitic magma.

INTRODUCTION

The Arabian-Nubian Shield (ANS) is a patchwork of microplates that are sutured along linear belts of ophiolites [1,2,3] and was evolved and cratonised during the late Precambrian Pan- African event (ca 1100-450 Ma, {4} . The basement complex in the ANS is characterised by the abundance of volcanosedimentary successions of greenschist facies metamorphism, dismembered ophiolitic complexes, gabbro-diorite-tonalite complexes and unmetamorphosed volcanic and pyroclastic sequences that are extensively intruded, particularly in the northern Egyptian Shield, by batholithic granodiorite-granite complexes {5, 6}

The metasediments in the Egyptian basement complex can be classified into three main types, oceanic, island-arc and continental metasediments. The first type have been interpreted as deep water deposits {7} and is mainly associated with pillow basalts without terrigenous sediments {7,8}. The island-arc metasediments, equivalent to those produced in the present day intra-oceanic isaland arc environment {4,9} consist maily of greywacke with less than 10% detrital K-feldspar {7}. The continental metasediments were termed the Igla formation by {5} and {10}. They are composed of a thick succession of coarse-grained and poorly sorted immature clastic sediments.

The gabbroic rocks of the Egyptian basement complex have different ages and tectonomagmatic evolution. The precambrian belt of the Egyptian basement contains two essential gabbroic types, namely older and younger gabbros. The first type is known as the El-Sid metagabbros {10} which includes metagabbro, amphibolite, meta-appilite, metanorite and metadolerite. These rocks have shown similarities with ophiolitic gabbros {11, 12, 13, 14, 15, 16}. The younger gabbros, on the other hand, considered to represent a late phase of calc-alkaline magma activity, are coeval with the Andean-type calc-alkaline magmatic rocks {17,18}. They are mostly fresh, unmetamorphosed and consist of norite, gabbro-norite, olivine-gabbro and troctolite {19}. The alkaline gabbro (troctolite) have been interpreted as post-tectonic, rift related intrusions {20}. Recently, {21} classified the Egyptian gabbroic rocks into island-arc (I-type), ophiolitic (O-type) and younger (Y-type) gabbros. Both the ophilitic and younger gabbroic suites have restricted compositions, gabbroic types commonly dominating. The island-arc (nonophilitic) intrusive metagabbro suites exhibit wide compositional variation and display more extreme fractionation trends with evolution towards tonalitic compositions {21}.

Two major volcanic episodes have been recognized in the precambrian crust of the Nubian shield. The products of early Pan-African volcanism (950-750 Ma; {22}) is represented by the Shadli metavolcanics which was subdivided by {8} into older metavolcanic rocks (ultramafic rocks and pillow basalts) and younger metavolcanic rocks (dominantly andesites and volcanogenic metasediments). The volcanic episode was succeeded by a younger Pan-african volcanic cycle (680-550 Ma; {22}) which produced voluminous volcanic assemblages, referred to as the Dokhan volcanic rocks {5,23}

With respect to the Egyptian granitoids, they were classified, generally, into older and younger granitoids {10, 15, 24 }. Recently , {25} classified the younger granitoids into orogenic I-type arc related, orogenic A-type arc-related orogenic A-type rift-related and anorogenic A-type rift-related granites. The older granitoids were considered to be mantle derived while the younger granitoids were derived by the partial melting of lower crustal rocks {26, 27, 28 }.

The aim of this study is to use petological and geochmical data to interpret the tectonomagmatic evolution of the rock assemblages encountered in the Zabara district.

LITHOSTRATIGRAPHY AND GEOLOGICAL SETTING

The Zabara district, covering an area of about 165 km2, is situated in the Central Eastern Desert of Egypt with coordination: long 34° 40' - 34° 46' E and lat. 24° 44' - 24° 49' N (Fig. 1). Different varieties of Precambrian rocks are represented in the Zabara district including metasediments, ultramafic / mafic rocks mainly serpentinites, ophiolitic metagabbro, ophilitic basic metavolcanics and non-ophiolitic intermediate to acidic metavolcanics and younger granite. The ophiolitic metavolcanics, metgabbro and serpentinite are thrusted over the metasediments. It is

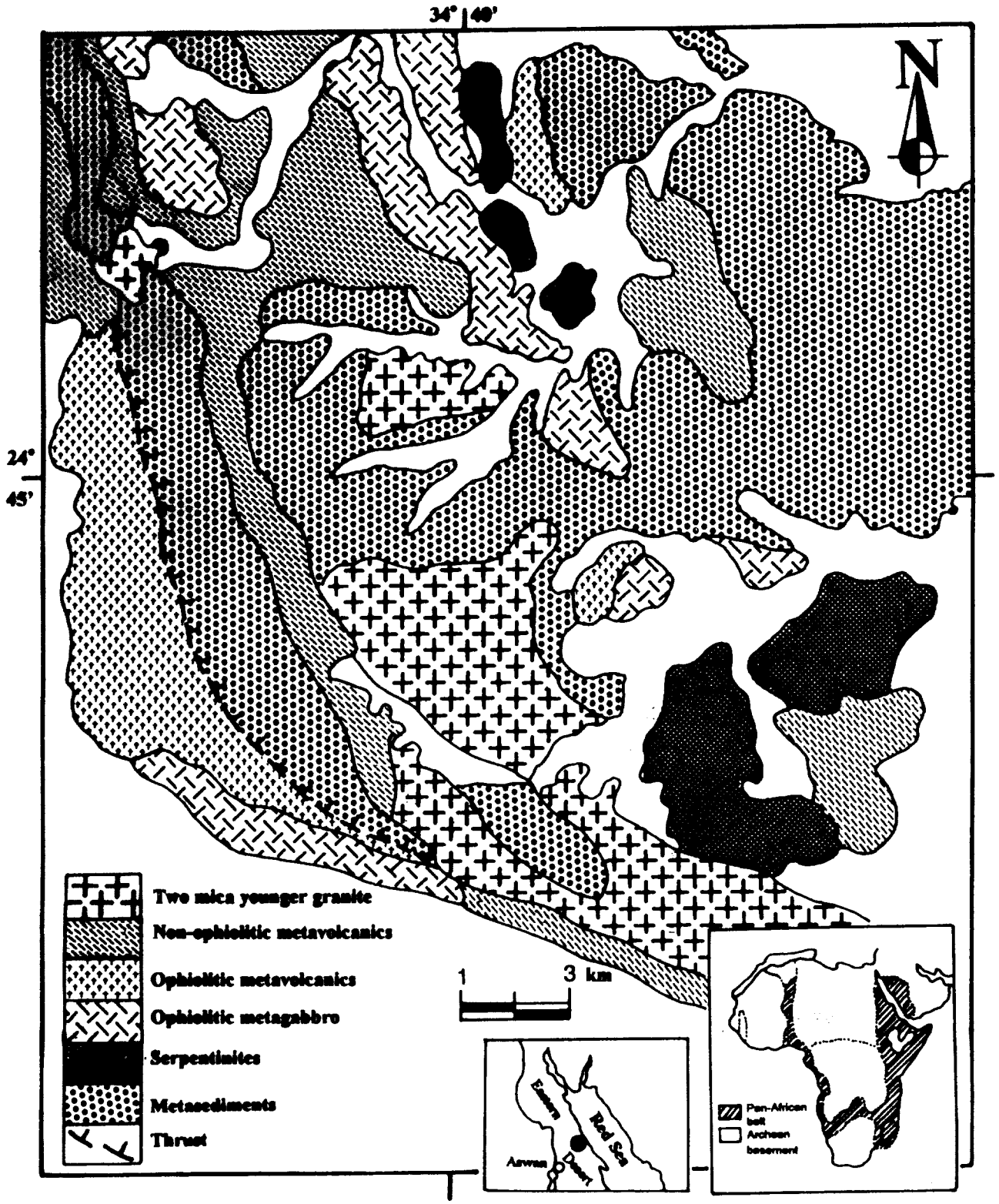

Figure 1: Geological map of the Zabara district. Inset maps show the location of the Zabara district in Egypt, and the geographical distribution of the Pan-African belt in Arabia and Africa.

apparent from the general structural attitude of the major rock units that the metasediments and the structurally overlying ophiolite, non-ophiolitic metavolcanics and volcaniclastic were folded together into major open folds {29}.

The matasediments are composed essentially of metagrewacke and metamudstone. These rocks are characterised by slump structures, scarcity of conglomerates and absence of calcareous beds suggesting their moderate to deep water depositional environment. The clastic fragments in the metagrewacke include volcanic rocks, gabbro, quartz and feldspars. The clastic fragments are mostly unaltered while the fine matrix is variably transformed into sericite, chlorite, epidote and actinolite. The metamudstone is very thinly laminated and composed mainly of quartz and feldspars with subordinate chlorite, muscovite and clay minerals. In some places, the metagreywacke and metamudstone are strongly sheared. The metasediments range in metamorphic grade from the lower greenschist facies up to the medium amphibolite facies.

The metagabbros, distinctly metamorphosed to greenschist facies, show most of the field characteristics of ophiolites according to the criteria of {30}. They are associated with srpentinites and lie tectonically on the underlying metasediments. The outcrops of the serpentinites, intensively altered to talc-corbonated along thrust faults, show no signs of thermal metamorphism against the host rocks suggesting that they are allochthonous and tectonically emplaced. The ophiolitic metagabbros, present as elongated masses trending mainly in a NNW direction, are heterogeneous in terms of mineralogical composition, texture and color index. They consist of layered and massive varities, with the latter being the main rock variety. The former is mostly restricted to the contact with the ultramafic rocks.

Two common metavolcanic rock types are distinguished in the Zabara district. These are (i) ophiolitic basic metavolcanics and (ii) non-ophiolitic intermediate to acidic metavolcanics. The ophiolitic metavolcanics are composed of a thick succession of metabasalts and from moderately elevated mountanous ridges with well developed jointing and faulting. They are green to greyish green in color, massive and fine-grained, yet porphyritic and amygdaloidal textures are frequently common. Their metamorphic grade range from the greenschist to the amphibolite facies. These rocks are thrusted over the ophiolitic serpentinites and ophiolitic metagabbros. The thrust is a narrow shear zone characterized by an abundance of broken blocks and cataclastic fragments, trending NW and dipping NE. It separates the ophiolitic metavolcanics from the underlying metasediments. The non-ophiolitic metavolcanics range in composition from meta-andesite through metadacite to site metarhyolite. They show porphyritic and amygdaloidal textures. The contacts of ophiolitic metavolcanics against the non-ophiolitic metavolcanics are often poorly defined. The metavolcanics are folded into a series of asymmetrical synclines and anticlines whose exial planed trend NNW-SSE {29}.

The younger two-mica granite typically displays sharp and non-reactive contacts against the surrounding rocks and is devoid of xenoliths. It is a medium-to coarse-grained with a marked equigranular texture but with occasionally gneissose texture with pink to red color. Small hematic cubes are occasionally present in the granite. According to the field relationship, the younger two-mica granite cross-cut virtually all the crystalline rock types encountered in the investigated area suggesting it younger age.

PETROGRAPHY

76 Samples representing the different rock types of the Zabara district were collected and petrographically examined in thin section.

Metasedimetns

The metasediment sequence is composed mainly of metagreywacke and metamudstone. The former is the most abundant and widespread. The metasediments are massive and frequently exhibit schitose textures with green greenish grey, dark grey and black colours. The metagreywacke is composed principally of quartz, albite and lithic fragments packed and scattered in a much finer matrix formed of silt and clay-sized clasts.

The detridal clasts are angular to subangular and rarely subrounded, and consist mainly of quartz, albite and rock

fragments intermixed in different proportions. Quartz is the most common mineral and usually forms monocrystalline grains with undulose extinction and polycrystalline fragments composed of numerous elongated to irregular crystals with sutured contacts. In the schistose varities, quartz grains are roughly elongated with preferred orientation parallel to the schistosity planes.

Plagioclase usually forms angular to subangular elongated and equidimentional clastic grains. It ranges in composition from plagioclase to albite and exhibits varying degrees of alteration, from olightly kaolinitised grains to completely altered ones. Occasionally, feldspar grains are replaced by the matrix minerals.

Lithic fragments occur in sandy and pebbly sizes and include wide varities of reworked mudstone, basalt, andesite and felsite.

The matrix is dark, lightly cementing the clastic grains. It is mostly muddy and consists of mixture of silt-and clay-sized grains of quartz, feldspar, chlorite, sericite, biotite, epidote and iron oxide, together with dark grey clayey materials.

The metamudstone is very fine-grained, mostly greenigh grey to dark grey colours. It consists of an extremely fine-grained mixture of different proportions of silty and clayey particles with or without minor amount of sandy grains. The clay fraction consists of aggregates of clay materials which is not amendable to thin section study. The silty fraction is made up of quartz, feldspar, white mica and opaques, while the sandy fraction is present in small amounts as subangular fine to very fine sandy grains of quartz and feldspar.

Ophiolitic metagabbros

The metagabbro is medium to fine-grained, equigranular and consists of plagioclase, augite and hornblende as principal phases. Alteration products are chlorite, clinozoisite and epidote while opaques, sphene and apatite are accessories.

Plagioclase ($An_{62,71}$) occurs as euhedral to subhedral prismatic to tabular crystals. Saussuritization, sericitisation and epidotisation are common. These alterations commonly vary from slight cloudiness at the core of the crystals to the development of dense aggregations of sericite, epidote and zoisite. Relatively fresh plagioclase crystals show complex albite and Carlsbad twinning. Cracking and bending of twin lamellae are occasionally recorded as signs of deformation.

Augite is present as subhedral crystals of comparable size to those of the plagioclase. Alteration to actinolite is common, especially along the margins. Hornblende forms ragged prismatic crystals and contains poikilitic inclusions of minute plates of plagioclase and apatite. Sometimes, hornblende is altered partially or completely to chlorite, epidote and actinolite. Occasionally, actinolite is present as fine acicular needles or as radiating fibers.

Ilmenite and titanomagnetite were studied in polished sections. A myrmekitic intergrowth between ilmentite and the silicate minerals is sometimes observed. Occasionally, ilmenite is altered along the periphery to rutlile and hematite. Unexsolved titanomagnetite crystals occurring as cubic, discete grains disseminated in the rock are rarely observed. Apatite inclusions are common in plagioclase and hornblende crystals.

Ophiolitic basic metavolcanics

The ophiolitic metavolcanic is mainly of basaltic composition. It shows porphyritic and amygdaloidal textures. The amygdales possess subspherical to elliptical shape filling with epidote, chlorite and calcite. The main constituents in the ophiolitic metabasalt are plagioclase, augite and hornblende. Secondary minerals include chlorite, actinolite and epidote. Opaques and apatite are the main accessories.

Plagioclase (An_{55-65}) occurs as idiomorphic to subidiomorphic phenocrysts as well as small laths in the groundmass. Low temperature alteration caused the cloudy appearance of plagioclase by secondary formation of sericite, epidote, clinozoisite and calcite. Relatively fresh phenocrysts exhibit lamellar twinning. Few plagioclase crystals show signs of deformation such as cracking and bending of the twin lamellae.

Clinopyroxene of augitic composition if present as subidiomorphic prismatic phenocrysts and as microlites in the groundmass. Alteration of augite begins along the grain margins and/or the cleavage planes, and frequently the

whole crystals are completely replaced by green actinolite and minor chlorite.

Hornblende phenocrysts are less abundant than plagioclase and augite. They occur as prismatic crystals, occasionally twinned and variably altered to chlorite and epidote.
Chlorite is the most dominant secondary mineral in the groundmass, whereas primary matrix phases like plagioclase, augite and hornblende are rarely preserved. Chlorite, actinolite and epidote occur as irregular patches and shredly aggregates. Opaques and apatite needles are variably represented in the groundmass.

Non-ophiolitic metavolcanics

The non-ophiolitic metavolcanics comprise of meta-andesite, metadacites and metarhyolites. They are pale green, greyish green, brown and reddish brown in colours. This rock association exhibits porphyritic and sometimes vesicular textures. Despite greenschist facies metamorphism of these rock types, they still contain primary igneous minerals which are fresh or partly subjected to secondary alteration. Plagioclase, hornblende, augite, biotite and quartz are the principal constituents of these rocks. Actinolite, chlorite, epidtote and zoisite are the alteration products while iron oxides and titanite are the accessories.

Plagioclase is mainly adnesine (An_{36}) in the meta-andesites and becomes more sodic in metadacites and metarhyolites with oligoclase to albite composition (An_{28-10}). Generally, the plagioclase forms idiomorphic to subidiomorphic tabular phenocrysts which are commonly twinned according to the Carlsbad, albite and multiple twinning laws. In some instances, the plagioclase phenocrysts are slihgtly to moderately altered to zoisite, epidote, sericite and calcite which often partially mask twinning. Furthermore, the phenocrysts are frequently deformed as indicated by the presence of undulose extinction and bending of the twin lamellae. Minute laths and microlites of plagioclase from the major part of the groundmass.
Primary hornblende phenocrysts mainly occur in the meta-andesites and to a lesser extent in the metadacites. They exhibit simple and polysynthetic twinning and alteration to epidote, zoisite and/or chlorite aggregates. Occasionally, some hornblende phenocrysts are bunched in aggregates forming a glomeroporphyrtic texture. Secondary actinolite after hornblende is observed as fibers that from pilotaxitic texture with plagioclase laths and quartz grains of the groundmass. Relict augite is rare in the meta-andesites, occurs as corroded boundaries phenocysts and exhibits partially and/or completely alteration to actinolite and chlorite.

Brownish-yellow shreds biotite are mainly recorded in metarhyolites and metadacites with subordinate amounts in the meta-andesites. The biotite shows pleochroism with formula: X (yellow) < Y ≤ Z (reddish brown). Some crystals are found to be altered partially and/or completely to chlorite.
Quartz is the most abundant constituents in the metarhyolites and, to a lesser extent, in the metadacites and meta-andesites. It occures as subidiomorphic phenocrysts as well as microlites in the groundmass. The phenocrysts exhibit wavy extinction with sharp contacts against the groundmass componets.
Opaques are the most common accessory minerals with subordinate of titanite. They occur as fine grains and pigments distributed in the groundmass and commonly associated with altered hornblende and biotite crystals.

Younger two-mica granite

The younger granite consists of quartz, potash feldspar, plagioclase, muscovite and biotite as essential minerals, while sericite, epidote and chlorite are the alteration components. Accessories includes apatite, titanite and zircon.
Quartz is the most abundant phase in the two-mica granite and present either as coarse-grained crystals or interstitial aggregates filling the interstices between the other constituents. The coarse-grained crystals are mostly euhedral to subheral and occasionally, show wavy extinction. Sometimes, quartz occurs as inclusions in plagioclase and biotite crystals or forms micrographic intergrowth with K-feldspar.
Potash feldspars occurs mainly as subhedral prismatic crystals of microcline and rare orthoclase. They are in most cases perthitic (patchy perthites). Rarely, the perthitic albite shows simple twinning. In some cases, alkali

feldspar is present as inclusions in the plagioclase forming antiperthitic texture.

Plagioclase (An_{23-13}) usually form euhedral to subhedral tabular and prismatic crystals. It is twinned according to the Carlsbad, albite and multiple laws. Some crystals show alteration to sericite and epidote. Occasionally, few crystals display zoning, resorbed boundaries and bending of twin lamellae. Inclusions in plagioclase are mainly represented by quartz, muscovite, epidote and opaques.

Muscovite occurs as euhedral to subhedral flakes. The large muscovite crystals are characterised by wavy extinction, bending of cleavage and common presence of opaques along cleavage planes. Biotite forms as short prismatic pleochroic euhedral to subhedral flakes. It is partially or completely altered to green chlorite. Inclusions of zircon, apatite and epidote are common in biotite.

Prismatic crystals of minute needles of apatite are disseminated in the granite as well as inclusions in biotite and plagioclase. Ilmenite form dark irregular grains usually associated with biotite flakes. Titanite occurs either as thin rims around titaniferous opaques or as subheral crystals always associated with biotite. Zircon inclusions surrounded by pleaochroic haloes are common in biotite.

GEOCHEMISTRY

Analytical techniques

Fourty one samples (5 ophiolitic metagabbros, 5 ophiolitic metabasalts, 4 meta-andesites, 4 metadacites, 4 metarhyolites, 13 younger granite, 3 metagreywackes and 3 metamudstones), crushed in an agate mortar, were analysed for major and trace elements. All whole-rock analyses were carried out at the institute of Mineralogy, Petrology and Economic Geology, Tohoku University, Japan. Major elements were determined of fused-glass discs, trace elements on pressed powder pellets, by a fully automatized Rigaku 3080E2 X-ray fluorescence spectrometer (XRF). Precision for major elements is better than 1% and around 10% for the trace elements. 12 samples were analysed for REEs by instrumental neutron activation analysis (INAA) (note that La, Ce and Nd values reported for samples without full REE analyses are values obtained by XRF).

Alteration effects

Petrographic studies indicate that the investigated metavolcanic units encountered in the Zabara district have been altered and matamorphosed to a greenschist to amphibolite mineral assemblage, with little retention of primary mineralogy. Alteration is substantially less pronounced in the younger two-mica granite, and primary minerals are preserved in many samples. The effects of alteration and metamorphism upon the remobilisation of elements should be cited in order to put constraints on, and justify the use of elements in petrogenetic considerations.

For major elements, {31} reported loss of CaO and Al2O3 during spilitization, and that SiO2, FeO* and Na2O may or may not be gained. During low-temperature alteration of basalts, the FeO*/MgO ratio, useful as a measure of differentiation, will increase, whereas SiO2 will b decreased {32, 33, 34}. Zielinski {35} showed that SiO2 and Al_2O_3 remained nearly unchanged, whereas the FeO/*MgO ratio was strongly depleted during the alteration of felsic rocks.

The mobility of the low-field-strength elements (LFSE) such as Cs, K, Rb, Ba and Sr is well documented, since these are rather sensitive to sea-water basalt interaction {36, 37, 38}. Therefore, major and LFS elements should be excluded or used with caution during any petrogenetic interpretation.

In contrast to the major and LFS elements, there is substantial agreement among geochemists that the high-field-strength elements (HFSE) like P, Ti, Y, Zr, Nb, Hf, Ta, Th, the transition elements (TE) like V, Cr, Co, Ni and REE are essentially immobile during alteration and metamorphism of the rocks {39, 40, 41, 42, 43, 44, 45, 46,

47}. Therefore, the immobile elements (TE, HFSE and REE), will be used largely for tectonomagmatic interpretation.

Major and trace element characteristics

Metasediments

The finer grained meta-clastic (metamudstones) show similar geochemical characteristics to the associated metagreywackes. However, the metamudstones have contents of SiO2. The Zabara metasediments, on the whole, are felsic and compositionally restricted in terms of major oxides with SiO2 (67.7% - 72.3%), Al2O3 (12.3%-15.4%), Fe2O3* (2.4%-5.9%), and MgO (0.96%-1.7%). The metasedimentary rocks are characterized by high Na_2O and K_2O contents, hence they plot in the field of sodic sandstone in the $(Fe_2O_3^* + MgO)$ - Na_2O-K_2O triangular diagram of {48} and in the compositional field of greywacke according to the classification of {49}. The relatively high SiO_2/Al_2O_3 and low K_2O/Na_2O (< 1) also favor a greywacke affinity. Although it is possible that the later ratio may have decreased due to the K-loss during weathering, low value of the Chemical Index of Alteration (CIA) (CIA = 100* Al_2O_3/ $(Al_2O_3 + CaO + Na_2O + K_2O)$ in mole %) ranging from 48.5 to 52.9 do not favor significant K-loss, which would raise CIA indices. The metasediments have low levels of V, Ni and Zn and moderate to high values of Sr and Ba (Table 1).

Table 1

Whole-rock chemical compositions for the rock associations of W. Zabara area, Eastern Desert, Egypt.

Sample #	YG-1	YG-2	YG-3	YG-4	YG-5	YG-6	YG-7	YG-8	YG-9	YG-10	YG-11	YG-12	YG-13	omg-14	omg-15	omg-16	omg-17	omg-18	omb-19	omb-20	omb-21
Type	Younger two-mica granites													Ophiolitic Metagabbros					Ophiolitic Metab		
Major elements (in wt.%)																					
SiO_2	74.06	77.17	72.61	72.74	72.43	72.66	72.95	72.78	72.72	75.67	73.90	72.30	74.30	48.34	50.65	51.77	48.33	47.85	51.23	48.83	52.01
TiO_2	0.05	0.04	0.21	0.11	0.11	0.06	0.07	0.06	0.07	0.05	0.22	0.22	0.06	1.43	1.51	1.39	1.49	1.36	1.34	1.45	1.52
Al_2O_3	15.62	14.04	14.96	14.69	15.72	15.51	15.31	15.23	15.24	14.32	14.04	15.31	15.57	13.48	13.67	13.35	14.05	13.89	15.93	15.27	14.73
Fe_2O_3	0.49	0.17	1.03	0.85	0.82	0.74	0.81	0.81	0.84	0.21	1.13	1.12	0.54	3.52	3.55	3.82	4.46	4.15	2.64	3.66	3.55
FeO	0.54	0.19	1.14	0.94	0.90	0.82	0.90	0.89	0.92	0.23	1.25	1.23	0.60	6.63	6.11	5.96	7.32	7.19	6.82	7.81	5.92
MnO	0.02	0.02	0.05	0.03	0.01	0.01	0.02	0.02	0.03	0.01	0.03	0.04	0.03	0.33	0.23	0.20	0.22	0.20	0.14	0.11	0.15
MgO	0.11	0.09	0.24	0.16	0.11	0.06	0.09	0.06	0.06	0.04	0.15	0.22	0.09	11.20	10.22	9.23	10.69	11.21	7.54	7.99	6.13
CaO	0.03	0.03	0.14	0.21	0.06	0.07	0.06	0.11	0.12	0.16	0.30	0.19	0.06	12.36	10.79	9.68	11.54	12.17	9.33	8.84	8.76
Na_2O	4.60	6.03	4.19	4.32	5.11	5.74	4.21	5.05	4.84	5.16	4.14	4.32	3.92	1.19	1.05	2.39	1.23	1.00	2.85	3.11	3.51
K_2O	3.09	1.48	4.91	4.47	3.50	3.37	4.64	3.67	3.88	2.97	3.61	3.90	4.16	0.26	0.21	0.33	0.29	0.42	0.22	0.28	0.30
P_2O_5	0.02	0.02	0.06	0.03	0.03	0.03	0.02	0.02	0.02	0.02	0.06	0.06	0.03	0.02	0.06	0.05	0.04	0.03	0.09	0.11	0.13
L.O.I.	0.99	0.59	0.69	0.90	1.10	0.73	0.60	0.98	1.02	0.87	0.79	0.61	0.38	0.97	0.75	1.72	0.89	1.00	1.67	2.35	2.38
Sum	99.64	99.87	100.23	99.45	99.90	99.82	99.68	99.68	99.76	99.71	99.62	99.52	99.74	99.73	98.80	99.89	100.55	100.47	99.80	99.61	99.09
Trace elements (in ppm)																					
V	n.d.	n.d.	n.d.	n.d.	n.d.	n.d.	n.d.	n.d.	n.d.	n.d.	n.d.	n.d.	n.d.	201	268	155	323	265	275	321	401
Cr	34	15	14	16	18	16	18	15	17	16	11	15	20	308	243	188	253	424	222	298	342
Co	n.d.	n.d.	3	n.d.	n.d.	n.d.	n.d.	n.d.	n.d.	n.d.	3	3	n.d.	58	55	68	66	76	64	59	72
Ni	8	8	11	8	11	9	7	7	7	7	8	8	8	141	143	175	210	189	88	143	99
Cu	7	7	6	8	11	12	11	48	41	8	12	11	37	50	87	61	73	43	75	64	98
Zn	76	4	205	267	138	93	129	27	40	30	570	605	52	60	66	49	59	51	92	100	54
Rb	162	138	190	211	100	161	267	200	213	148	145	149	262	4	6	5	6	4	4	6	4
Sr	34	61	67	31	95	99	23	41	41	47	60	63	38	147	166	162	218	177	103	194	188
Y	72	22	64	62	39	44	42	61	56	40	62	59	76	23	28	39	29	32	33	38	42
Zr	315	199	240	154	173	224	174	302	304	126	263	243	250	77	72	63	91	87	104	121	86
Nb	102	86	68	81	76	74	90	113	119	85	76	81	72	5	4	5	5	7	5	5	7
Ba	106	146	160	129	119	112	111	91	92	70	196	190	121	57	45	61	84	73	35	42	73
La	***46***	41	39	34	43	32	44	***49***	42	32	***61***	61	50	***2.9***	n.d.	***2.6***	n.d.	n.d.	***8.4***	5	6
Ce	***118***	86	88	77	96	81	92	***97***	88	79	***130***	62	89	***8.5***	7	***8.1***	9	11	***22.2***	29	31
Nd	***43***	52	45	43	55	58	47	***36.8***	50	32	***48***	44	66	***5.7***	10	***5.1***	8	6	***12.3***	10	15
Sm	***8.3***							***9.5***			***11.5***			***2.2***		***2.1***			***3.9***		
Eu	***0.3***							***0.2***			***0.5***			***0.7***		***0.7***			***1.1***		
Gd	***3.2***							***3.8***			***3.9***			***2.8***		***2.6***			***5***		
Tb	***2***							***2.2***			***2.2***			***0.5***		***0.4***			***1.1***		
Ho	***n.d.***							***n.d.***			***n.d.***			***n.d***		***n.d***			***n.d***		
Tm	***n.d.***							***n.d.***			***1.3***			***n.d***		***n.d***			***n.d***		
Yb	***2.5***							***2.9***			***2.9***			***1.8***		***1.5***			***3.4***		
Lu	***0.8***							***0.8***			***0.8***			***0.3***		***0.3***			***0.6***		
Sc	***1.4***							***0.4***			***2.1***			***42.3***		***49.6***			***38.4***		
Hf	***8.6***							***16.4***			***9.5***			***2.4***		***2.6***			***2.9***		
Ta	***9.5***							***12.4***			***4.4***			***0.2***		***0.3***			***0.3***		
Th	***22.4***							***21.1***			***13***			***0.2***		***0.3***			***0.3***		
U	***5.5***							***4.7***			***3.1***			***n.d***		***n.d***			***n.d***		

Key: n.d. = Not detectable; L.O.I. = Loss-on-ignition; Italic bold = Analysed by INAA.

omb-22	omb-23	ma-24	ma-25	ma-26	ma-27	md-28	md-29	md-30	md-31	mr-32	mr-33	mr-34	mr-35	mg-117	mg-150	mg-151	mm-170	mm-103	mm-172
ssalts		Meta-andesites				Metadacites				Metarhyolites				Metagreywacke			Metamudstone		
50.25	52.91	58.95	57.77	60.53	55.95	67.34	63.17	68.72	65.71	73.03	70.16	72.33	71.71	71.31	71.91	72.32	69.00	68.77	67.42
1.27	1.39	0.85	0.71	0.54	0.77	0.45	0.58	0.41	0.52	0.13	0.22	0.11	0.15	0.45	0.22	0.23	0.25	0.51	0.58
16.21	15.73	12.79	11.62	11.87	12.49	13.52	14.71	13.99	14.06	15.66	14.68	15.82	15.59	13.84	13.96	12.26	15.39	13.32	13.68
2.93	2.95	4.23	3.45	2.55	4.29	2.05	2.04	1.89	2.44	0.61	1.04	0.81	0.76	1.35	1.97	1.84	0.67	1.69	2.00
6.61	6.20	5.20	5.33	4.91	5.11	3.17	3.14	2.76	3.65	0.68	1.14	0.76	0.84	1.87	1.22	1.66	1.55	2.23	3.51
0.12	0.11	0.13	0.13	0.14	0.11	0.18	0.20	0.15	0.15	0.06	0.11	0.05	0.06	0.10	0.14	0.14	0.08	0.16	0.19
5.85	5.83	7.36	8.61	8.86	7.67	1.50	1.48	1.21	1.60	0.31	0.25	0.38	0.15	0.87	0.62	0.87	0.96	1.12	1.72
9.71	8.49	5.84	6.87	6.12	7.25	4.02	4.37	3.92	3.76	0.51	0.58	0.71	0.47	2.45	3.39	3.08	3.39	2.99	3.16
3.53	2.81	3.04	3.31	2.99	2.65	4.06	4.40	3.65	3.93	4.49	4.20	4.14	4.42	4.46	3.28	4.84	4.61	4.47	4.21
0.21	0.31	0.96	1.21	1.00	0.74	3.39	3.43	2.10	3.74	4.22	4.46	3.98	4.42	2.65	0.78	0.89	1.53	0.90	0.94
0.15	0.13	0.22	0.04	0.02	0.03	0.21	0.15	0.19	0.27	0.03	0.07	0.06	0.05	0.09	0.03	0.06	0.06	0.11	0.10
2.82	2.77	0.83	1.52	1.11	2.44	0.52	1.63	0.82	0.6	0.75	1.81	1.34	0.89	0.55	1.86	1.29	1.87	2.76	2.86
99.66	99.63	100.40	100.57	100.64	99.50	100.41	99.30	99.81	100.43	100.48	98.72	100.49	99.51	99.99	99.38	99.48	99.38	99.03	100.37
365	293	95	106	89	132	71	56	66	62	n.d.	n.d.	n.d.	n.d.	58	32	45	40	57	107
361	273	56	123	80	176	66	71	55	42	25	21	17	15	33	54	61	46	60	53
43	66	15	20	18	21	21	16	18	15	5	4	6	2	6	7	8	6	10	16
207	152	66	74	58	78	17	20	12	10	10	8	6	8	9	12	12	13	24	25
105	55	39	44	53	30	42	63	59	66	29	26	31	19	14	18	58	31	33	31
53	62	47	48	33	51	98	80	121	109	51	66	59	31	23	15	22	33	78	75
7	4	30	33	28	37	41	51	47	46	41	44	55	49	36	12	15	25	21	21
199	132	353	397	442	476	306	230	266	295	83	67	100	65	191	222	194	400	172	201
35	32	41	48	39	45	39	33	26	29	32	20	37	25	26	18	17	27	36	25
92	83	196	233	228	265	264	215	261	234	221	205	199	176	100	81	62	107	124	104
4	5	13	12	10	15	22	18	21	15	52	66	61	67	6	3	n.d.	n.d.	5	3
29	53	482	463	585	430	332	292	351	352	320	330	315	285	650	221	347	479	275	136
6.9	10	***18.9***	23	26	20	44	***36***	39	41	55	***47***	50	43	12	***5.7***	n.d.	n.d.	11	***6.7***
24.6	25	***44.3***	53	49	44	82	***75***	71	66	110	***91***	98	101	24	***14.6***	13	17	23	***18.5***
15.1	18	***23.1***	29	33	37	33	***29***	35	28	42	***48***	44	40	11	***8.9***	8	9	19	***11.3***
4.9		***6.3***					***6.8***				***11.5***				***2.6***				***3.5***
1.5		***1.9***					***1***				***0.7***				***0.6***				***1***
5.4		***10.0***					***4.0***				***3.9***				***2.5***				***5.1***
1.0		***1.7***					***0.7***				***0.7***				***0.4***				***0.8***
n.d		***n.d***					***1.3***				***1***				***0.8***				***1.1***
n.d		***n.d***					***0.6***				***n.d***				***0.4***				***0.5***
2.7		***4.2***					***3.9***				***6.4***				***2.3***				***2.5***
0.4		***1.1***					***1.3***				***2.1***				***0.4***				***0.5***
41.5		***19.1***					***15.6***				***2.5***				***11.2***				***16.2***
3.3		***4.2***					***5.2***				***5.7***				***2.1***				***2.5***
0.4		***0.6***					***1***				***1.3***				***0.03***				***0.2***
0.4		***4.3***					***6.2***				***11.3***				***2.7***				***2.1***
n.d		***1.8***					***1.4***				***2.9***				***1.1***				***1.1***

Variation diagrams (Fig. 2) show that the major and trace elements of the metagreywacke and metamudstone are closely similar to the composition of metadacite metarhyolite and younger granite. The relatively low Cr and Ni contents of the metasedimentary rocks suggest that felsic lithologies (granite and/or felsic volcanics) predominate the mafic and ultramafic rocks in their source areas. However, the very low Th/U ratios of the Zabara metasediments relative to the investigated younger granite preclude the contribution of the latter to their source area. On the other hand, Cu/Zn ratios in the metasedimentary rocks and non-ophiolitic metavolcanics are closely similar suggesting that the latter being predominant rocks in the source area.

The Zabara metasedimentary rocks have a chondrite-normalized REE pattern characterized by slightly fractionated LREE, flat HREE and absence of an Eu anomaly (Fig. 3) similar to the pattern of the non-ophiolitic metavolcanics. However, the metasedimentary rocks have less fractionated and lower contents of LREE than the non-ophiolitic metavolacanics (Fig. 3). The sum of REEs contents increase from metagreywacke to metamudstone (39.2 and 51.5, respectively).

MORB and ORG after {86} and {64}, respectively. Thevalues of CIA (continental island arc greywacke); ACM (active continental margin greywacke) and PM (passive continental margin greywacke) are from {86}.

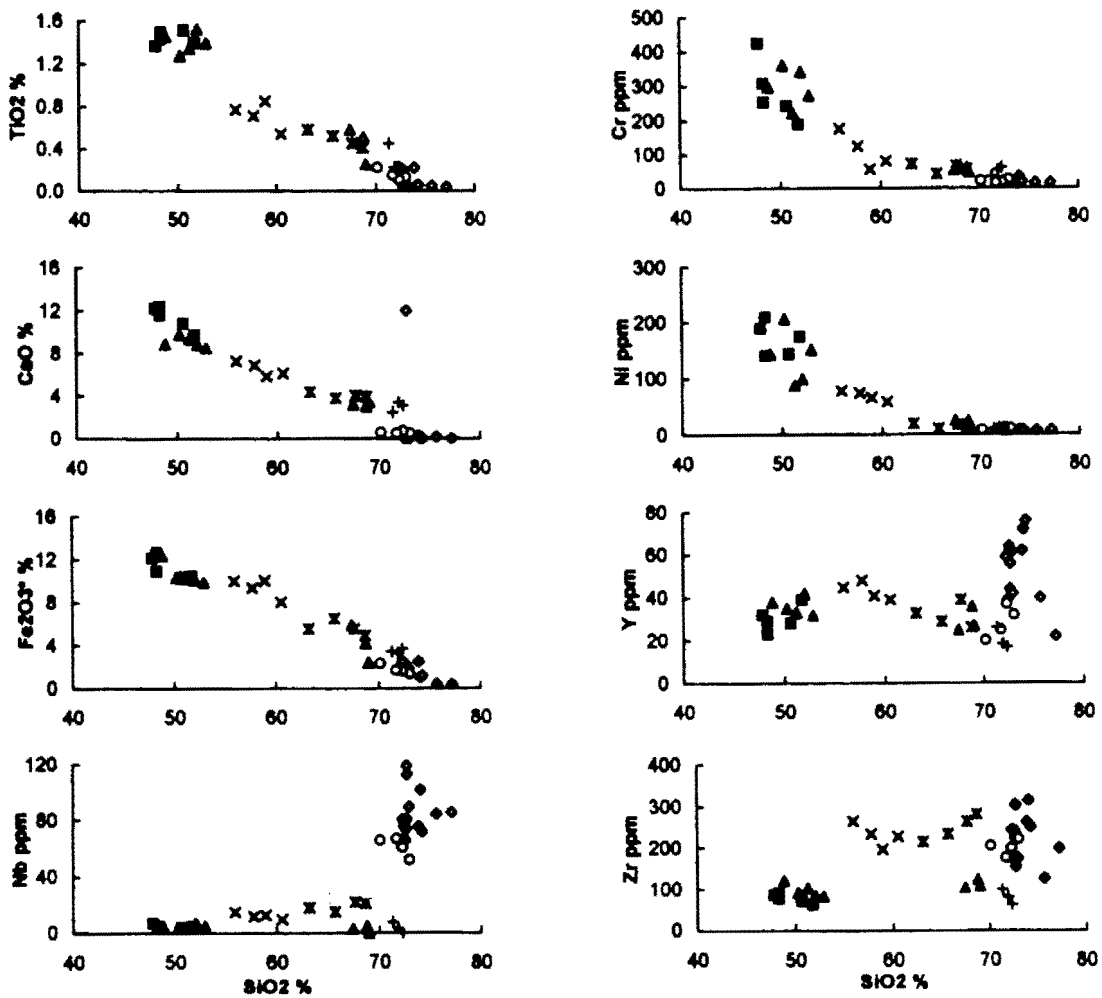

Figure 2: Selected Harker variation diagrams for major and trace elements from the Zabara district. Symbols: filled squares = ophiolitic metagabbro; fille triangles = ophiolitic metabasalt; cross = meta-andesites; astriskes = metadacites; open circles= rhyolites; rhombas = two mica younger granites; plus = metagreywakes; open triangles = metamudstones.

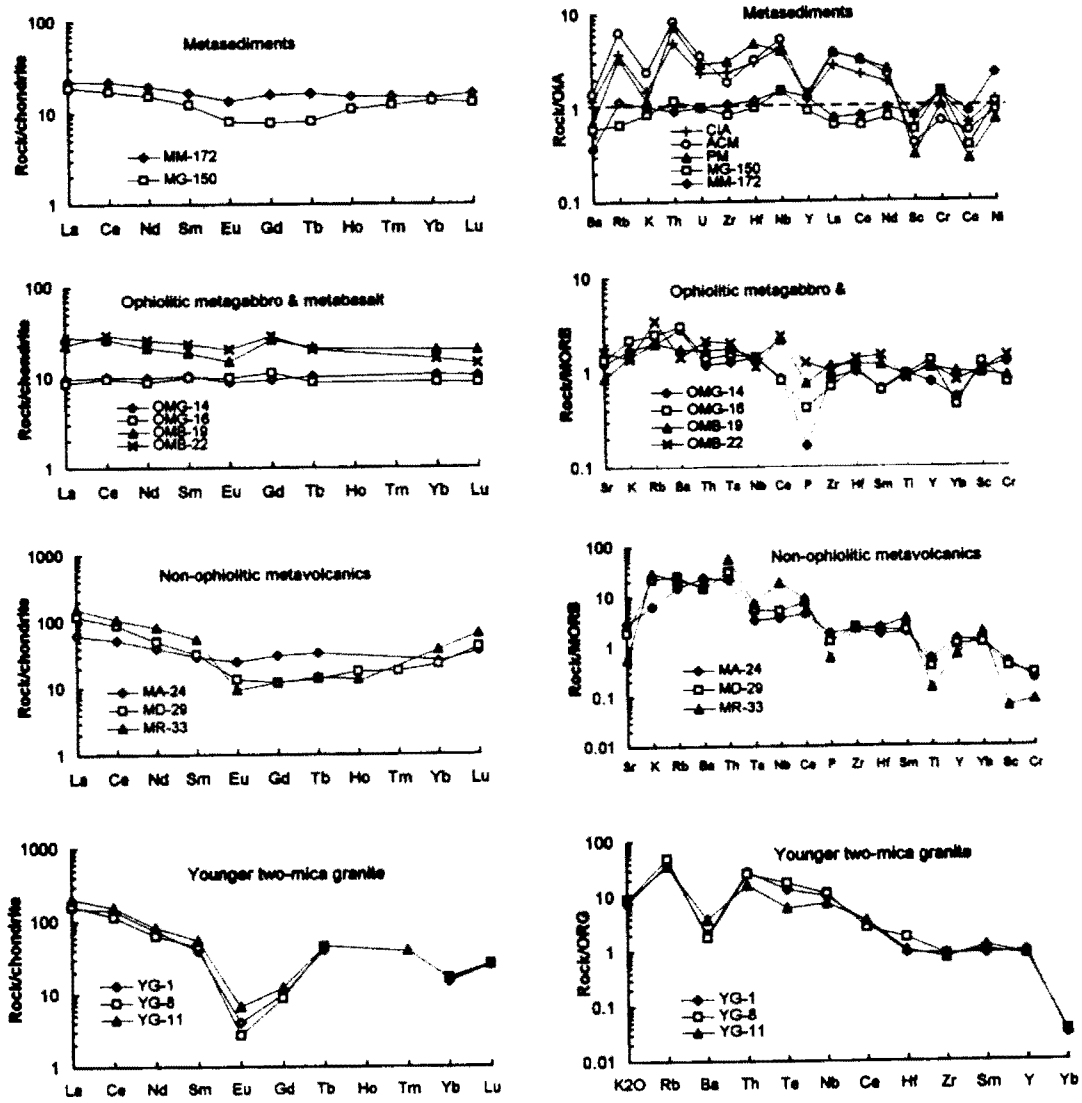

Figure 3: (a) chondrite-normalized rare earth element (REE) diagrams for the metasediments, ophiolitic metagabbros and metabasalts, non-ophiolitic metavolcanics and younger two-mica granites of the Zabara district. Normalization values after {82}. (B) OIA (oceanic island arc)- normalized multi-element diagram for the metasediments; MORB (mid ocean ridge basalt) - normalized multi-element diagrame for the ophiolitic metagabbros and metabasalts and the non-ophiolitic metavolcanics; and ORG (ocean ridge granite)- normalized multi-element diagram for the younger two-mica granites of the Zabara district. Normalization values of the OIA,

The chemical composition of sediments provides an important clue to their provenance and tectonic setting. {50} defined three types of sedimentary basins related to plate tectonic setting. These basins are (i) PM (passive margin)-basin on continental crust, and basins associated with ocean floor spreading, (ii) ACM (active continental margin)-subduction-related basins, continental collision basins and pull-apart basins associated with strike-slip fault zone and (iii) Arc-subduction-related basins. The major elements geochemistry of the metasediments gives insight to the tectonic setting of the basin in which they were deposited {51}. The SiO_2 vs K_2O/Na_2O diagram (Fig. 4) reflects that the investigated metasedimentary rocks were deposited in an oceanic island arc basin. The trace elements, particularly those which are relatively immobile, can also be very useful. Elements La, Ce, Nd, Y, Th, Zr, Hf, Nb, Ti and Sc are most suited for provenance and tectonic setting determinations because of their relatively low mobility during sedimentary processes and their low residence time in sea water {52}. These elements are transported quantitatively into clastic sedimentary rocks during weathering and transportation and thus would reflect the signature of the parent material {33}. The investigated metasediments are normalized to well known tectonic metasediments. Indeed, the OIA (oceanic island arc)-normalized spiderdiagram (Fig.3) shows that the metasediments are closely similar to those of the OIA metasediments.

Ophiolitic metagabbros and metabasalts.

These rocks are similar in both major and trace elements contents (Table 1) and therefore they will be discussed as a single unit termed hereafter as OMGB (OMGB = ophiolitic metagabbro and metabasalt). The SiO_2 contents range from 47.9 to 54 wt% and Mg-number (Mg# = 100 MgO/(FeO^* +MgO)) from 53.3 to 38.7. However, the ophiolitic metagabbro have higher Mg (ranging from 53.3 to 48.5 and from 45 to 38.7, respectively). MgO shows a wide variation ranging from 5.8 to 11.2 wt%, while TiO_2 reveals a restricted range (1.3 - 1.5 wt%). K_2O, P_2O_5 and the incompatible trace elements Zr and Y exhibit low concentrations (Table 1). The subalkaline affinity of the ophiolitic units are demonstrated by the Na_2O+K_2O vs SiO_2 plot {50} and by the P_2O_5 vs Zr digram {54}. The sample of these rocks plot in FeO*/MgO vs SiO_2 and TiO_2 diagrams {55} in the rather restricted field of tholeiite (Fig. 5A and 5B). Gelinas *et al* {56} have shown that the tholeiitic and clac-alkaline suites can be distinguished using incompatible element ratios such as Zr/Y and Ti/Zr. The ophiolitic metagabbros and metabasalts display Zr/Y < 4 (2.7 and 2.7, respectively and Ti/Zr > 70 (112 and 88, respectively) a feature typically characterised tholeiitic suites {56}.

Chondrite-normalized REE patterns of the metagabbros and metabasalts(Fig.3) are relatively flat with 10-20 chondritic abundances and characterized by absent to slightly negative Eu anomalies. The ophiolitic metabasalts have higher REE contents than the metagabbros. The enriched and unfractionated HREE in the metagabbros and metabasalts with average value of (Gd/Lu)n 0.87 and 0.95, respectively,) is inconsistant with the presence of residual garnet in the magma source.

The ophiolitic sequence is characterized by very low K_2O, Nb, Zr, Rb and Ba contents (Table 1) typically similar to N-MORB. Ti/V ratio of the metagabbros and metabasalts range from 20 to 50 suggesting their MORB affinity {42}. During the last decade, many attempts have been made to classify basalt compositions on the basis of their tectonic setting through various emperical diagrams {57, 58, 59, 60, 61}. On the Nb-Zr-Y ternary diagram of {61}, the investigated metagabbro and metabasalt samples plot closely in the N-MORB field. MORB-normalized patterns of the metagabbro and metabasalt (Fig. 3) are characterized by LILE-enriched relative to MORB and with strongly negative P anomalies in the metagabbro and less pronounced in the metabasalt.

Non-ophiolitic metavolcanics

Major elements analyses show that these rocks range in composition from intermediate to acidic (58.1-73 wt% SiO_2). On the SiO_2 vs. K_2O diagram {62} the non-ophiolitic metavolcanics are classified as meta-andesite, metadacite and metarhyolite (Fig. 6). The meta-andesite plots mainly in the medium-K calc-alkaline field while both the metadacite and metarhyolite plot in the high-K calc-alkaline field. These rocks display average Zr/Y > 4 (5.3, 8 and 7.4, respectively) and Ti/Zr < 70 (19, 12 and 5, respectively) suggesting their calc-alkaline

affinity {56}. Selected major and trace elements variation (Fe_2O_3*, CaO, TiO_2, Ni and Cr) plots vs. SiO_2 show a coherent curvilinear trends (Fig.2), suggesting the important role played by fractional crystallization in their generation.

Chondrite-normalized patterns for the meta-andesite, metadacite and metarhyolite are shown in Figure 3. The non-ophiolitic metavolcanics have similar chondrite-normalized patterns characterized by LREE-enrichement, with (La/Sm) N = 2.1 for meta-anesite, 3.7 for metadacite and 2.9 for metarhyolitic, and unfractionated HREE with (Gd/Lu)N = 0.9 for meta-andesite, 0.3 for metadacite and o.2 for metarhyolite. The meta andesites and metadacites are characterised by the absence of Eu anomalies, whereas the metarhyolite shows a slightly negative Eu anomaly suggesting plagioclase fractionation.

MORB-normalised spiderdiagrams of the non-ophiolitic metavolcanics (Fig. 3) are characterized by slightly negative P and Ti anomalies in the meta-andesite and metadacite. These anomalies are believed to be typically produced in an active margin settings due to LILE enrichment in the mantle wedge by fluids from the subducted lithosphere and the retention of some elements, eg. Nb, during magma separation {63}. The meta-andesites and metadacites are characterized by Ta-Nb negative anomalies suggesting their generation in a subduction-related volcanic are setting. The metarhyolites show high contents of Nb relative to the meta-andesites and metadacites which can be explained by the effect of crustal assimilation {64}. On the Nb vs Y binary diagram {64} the meta-andesites and metadacites plot mainly in the volcanic arc and sy-ncollision field while the metarhyolites plot in the within-plate field (Fig. 7). The low content of Rb/Zr for the meta-andesite and metadacite suggest a volcanic arc rather than a syn-collision setting (64).

Younger two-mica granite

Major, trace and REE composition of the younger two-mica granite are given in Table 1. On the ANOR-Q diagram (Fig.8), the two-mica granite is classified as alkali granite. The rock shows a wide variation in terms of K_2O (1.5-4.9 wt%), Rb (100-267 ppm), Y (22-76 ppm), Zr (126-315 ppm) and Nb (66-119 ppm) within a limited range of SiO_2 content (72.3-77.2 wt%). Major and trace elements plots vs. Sio_2 (Fig. 2) for the two-mica granite do not show a definite smooth variation trend. The Harker diagrams depicts the close similarity between the compositions of the metarhyolites and the younger two-mica granite, which may suggest that the granite represents the plutonic equivalent of the rhyolite.

The younger two-mica granite has agpaiitic index values (ranging from 0.7 to 0.9) characteristic for many alkaline complexes throughout the world {65}. The rock is characterised by high Fe-numbers of Fe# = FeO*/ (FeO*+MgO) with an average of 0.9 and can be classified as very Fe-rich granite according to the classification of {66}. The alumina saturation index ASI = Al_2O_3/ (Na_2O+K_2O+CaO) molar is high for the younger two-mica granites, ranging from 1.2 to 1.4 which classifies it as hyperaluminours granite according to the classification of {67}. Using the classification of {68,69} the younger two-mica granites can be classified as ferriferous, peraluminous leucocratic granite with muscovite > biotite.

The REE patterns of the two-mica granites (Fig. 3) display a gull-wing shape, moderately fractionated LREE, with (La/SM)u = 3.7, on average, and unfractionated HREE with $(Gd/Lu)_N$ = 0.4, on average. The patterns are characterised by pronounced negative Eu-anomalies.

The two-mica granite is characterised by high contents of SiO_2, alkalies, Rb and high field strength elements (HFSE) and low contents of MgO and CaO typically similar to A-type granites {70}. ORG (ocean ridge granite)-normalized spiderdiagram (Fig. 3) shows that the two-mica granite displays strongly negative Ba anomalies, whereas of negative Ta-Nb anomalies are absent suggesting a formation in a tensional tectonic environment {64}. According to the tectonic classification diagrams of the granitoids {64, 70, 71, 72}, the younger two-mica granites plot exclusively in the within-plate, A-type granite field. {72} classified the A-type granite into two subtypes namely: All-subtype (Y/Nb < 1.2) of anorogenic rift-related environment and A2-subtype (Y/Nb > 1.2) of post-orogenic subduction-related regime. The two-mica granites have Y/Nb < 1.2 suggesting its anorogenic rift-related environment {72}. However, the low Y/Nb

ratio for the two-mica granites can be attributed to the crystallization of amphibole and/or minor phases such as zircon and allanite, which will lead to a decrease in Y with respect to Nb {71}, thus lowering the Y/Nb ratio in the investigated granite. The high Fe# (0.9) for the granite is typical of post-tectonic environment rather than an anorogenic, rift-related regime {73}. Field relations, petrological and geochemical features indicate that the investigated granites, like other post-orogenic alkaline granites, are transitional between typical anorogenic alkaline granites and orogenic calc-alkaline granites of mature magmatic arcs.

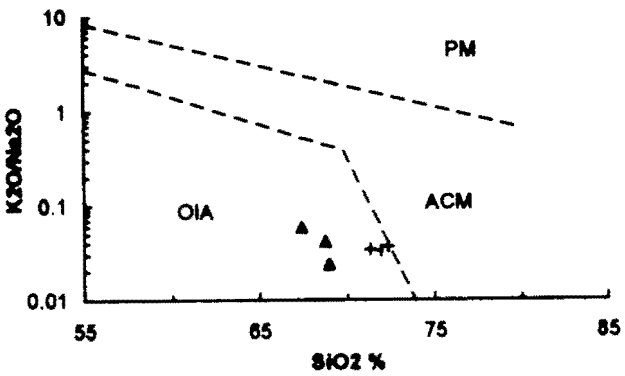

Figure 4: SiO_2 vs K_2O/Na_2O plot of the Zabara metasediments. Field boundaries for the various tectonic setting are from {50}. OIA = oceanic island arc; ACM = active continental margin and PM = passive continental margin. Symbols as in Figure 2.

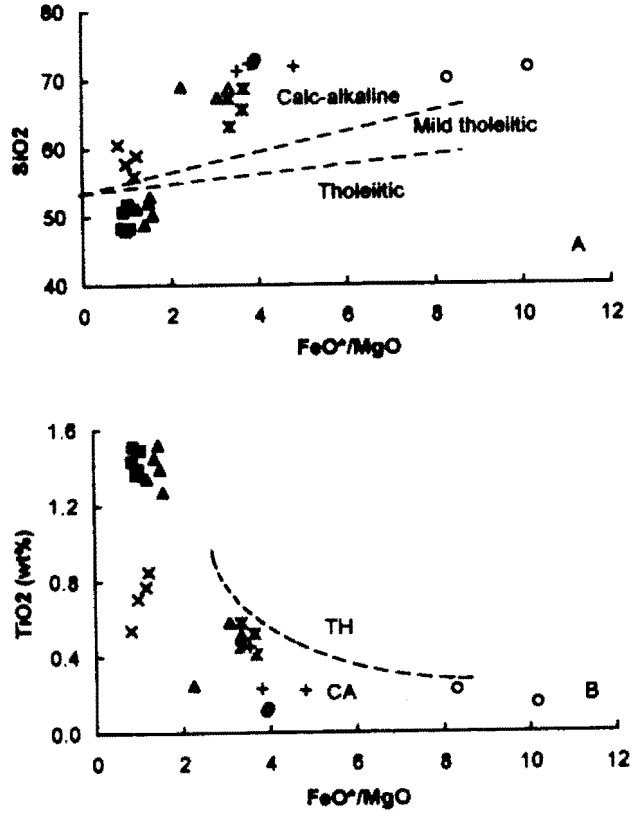

Figure 5: Feo*/MgO vs Sio_2 (A) and Tio_2 (B) showing the tholeiitic affinity for the ophilitic metagabbros and metabasalts and calc-alkaline affinity for the non-ophiolitic metavolcanics and metasediments. Lines separate calc-alkaline (CA) and tholeiitic (TH) fields are after (55). Symbols as in Figure 2.

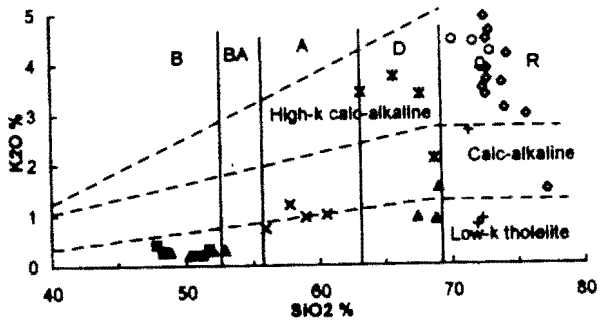

Figure 6: SiO_2 vs K_2O classification diagram after (62) for the different rocks of the Zabara district . B = Basalts; BA = Basaltic andesite; A = andesites; D = dacites; R = rhyolites. Symbols as in Figure 2.

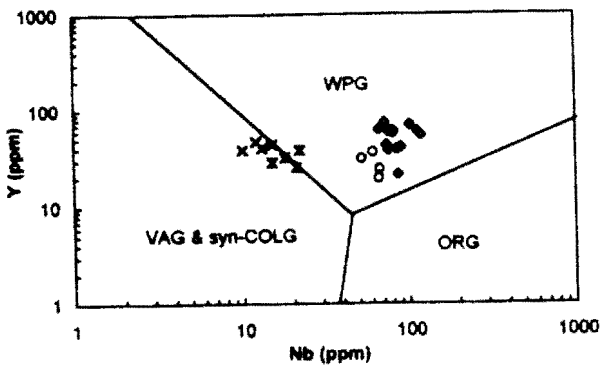

Figure 7: Nb vs. Y discrimination diagram for the non-ophiolitic metavolcanics and younger two-mica granites of the Zabara district. Fields of within-Plate granite (WGP), volcanic arc granite (VAG), syn-collision granite (syn-Colg) and ocean ridge granite (ORG) are from {64}. Symbols as in Figure 2.

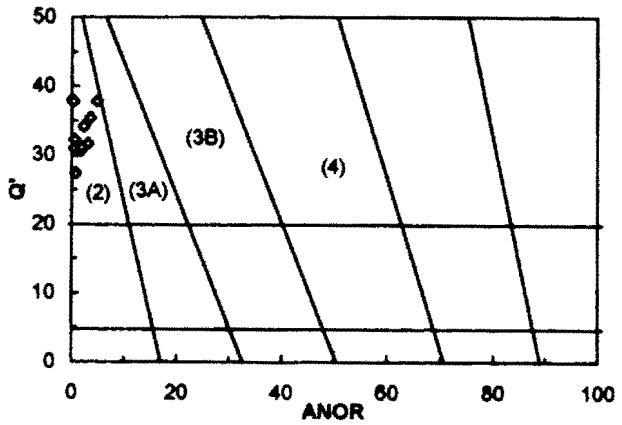

Figure 8: ANOR vs. Q' classification diagram of {88} for the Zabara two-mica granites. Q' and ANOR are calculated using the norm components as follows: Q' = Qz/(Qz + Or+ Ab + An) and ANOR = AN/ (Or + An). Normative fields are (2) alkali granites, (3A) syenogranite, (3B) adamellite and (4) granodiorite.

PETROGENESIS

The close similarity in the composition of both the ophiolitic metagabbro and ophiolitic metabasalt suggests that they generated from the same magma source. The Zr/Y vs. Nb/Y diagram (Fig. 9) supports the genetic relationship between the ophiolitic metagabbros and ophiolitic metabasalts where their samples plot in superimposed fields. The other different rock types show variations which suggest multiple parental magma sources and/or different melting proportions for the same source {74}.

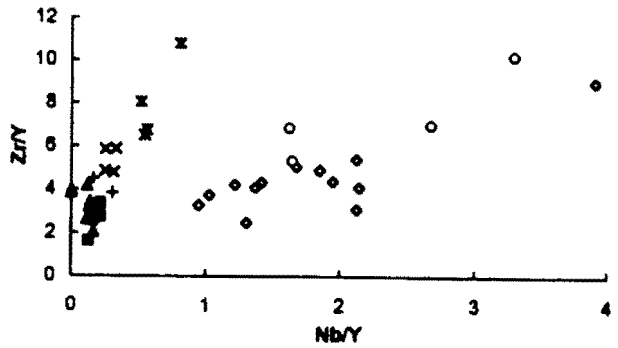

Figure 9: Nb/Y vs. Zr/Y diagrame for all rocks of the Zabara district. Symbols as in Figure 2.

The OMGB rocks exhibit a wide range of Mg-numbers, but low values (51 for the metagabbros and 41 for the metabasalts, on average) to be in equilibrium with the unmodified primitive mantle source (> 70 Mg#, {75}). The low Mg# and low contents of Ni and Cr of the OMGB rocks relative to primitive mantle source (> 250 ppm Ni and > 1000 ppm Cr, {75, 76}) suggest that some of the chemical variation in these rocks may be attributed to fractional crystallization, dominantly of olivine and pyroxene. On the other hand, the distinct geochemical features such as high MgO and FeO* and low Zr and Nb, combined with flat normalized REE patterns and high HREE of the OMGB are typical of a high degree of mantle melting of garnet-free source. The non-ophiolitic metavolcanics cover the entire spectrum from meta-andesite to metarhyolite. The smooth variations trends for major and trace elements (Fig. 2) and the patterns of the REE suggest that these rocks are comagmatic, and fractional crystallization process played a major role during their evolution. There is close similarity between the composition of both the metarhyolites and the younger two-mica granites. The metarhylites and the granites have similar ratios of ZR/Nb (3.3 and 2.7, respectively), Nb/Y (2.3 and 1.8, respectively) and Ti/Zr (4.6 and 2.8, respectively) which may suggest their generation from a chemically similar magma source.

To evaluate whether partial melting and/or fractional crystalisation was the dominant operating process, it is desirable to compare trends among incompatible and compatible elements {77}. The Y vs Cr diagram {78} is suitable for such an evaluation in metamorphosed mafic rocks since Y and Cr are among the immobile elements during alteration and metamorphism {79}. This diagram (Fig. 10) shows that the different rock types could have been generated by different extents of partial melting, with minor fractionation of clinopyroxene and/or hornblende as indicated by decreasing in Cr contents. Petrogenetic modelling using the Cr-Y covariation diagram (Fig. 10) indicate that - 10% partial melting is required to produce metabasalts and meta-andesites and - 25% partial melting to produce metagabbros. Conversely, the Cr-depleted characteristics of metadacite and metarhyolite indicate their derivation from magma that had undergone significant degrees of fractional crystallisation.

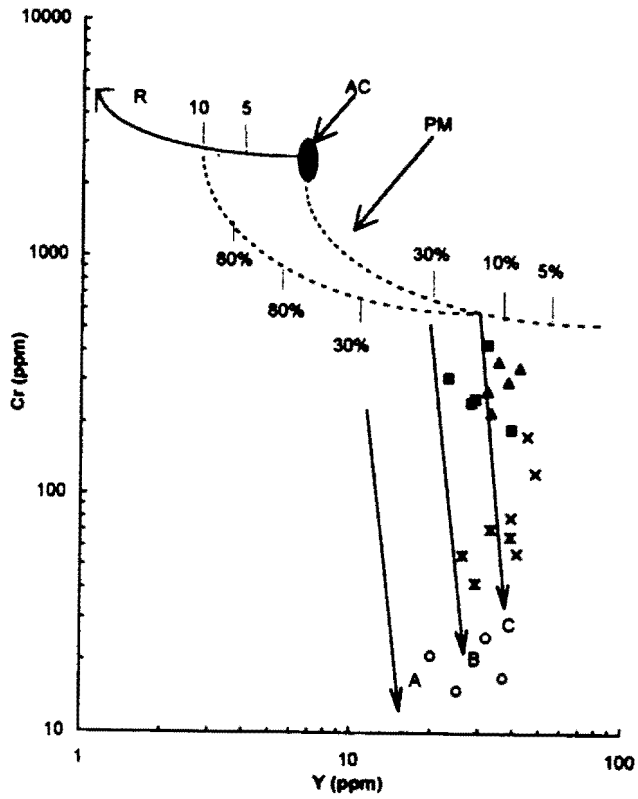

Figure 10: Y and Cr values for ophiolitic and non-ophiolitic metavolcanics, plotted on a diagram after {78}. R = residual oceanic lithosphere compositions; AC = asthenosphere compostion; PM=present the petrogenetic pathways of Boninitic suit, island are tholeiite and mid occean ridge basalt, respectively. Symbols as in figure 2.

The incompatible elements Zr and Y are generally enriched during fractionation. This can be observed in a diagram showing the Zr/Y ratio as a function of Zr concentration (Fig.11). On this diagram, a slight increase of the Zr/Y ratios in the metagabbros and metabasalts, reflects the incompatibility of Zr to the early fractionated phases, particularly clinopyroxene {59, 80}. The meta-andesites have a similar rate of Zr/Y increasing as for the OMGB, which may indicate clinopyroxene fractionation. This behaviour of Zr/Y suggests the common presence of clinopyroxene in the magma source (lherzolite) for the OMGB and meta-andesite. The metadacites and metarhyolites show a remarkable increase of Zr/Y which may emphasize the onset of amphibole fractionation, a mineral in which Y is strongly compatible (Kd = 2.5) and Zr is incompatible (Kd = 0.5) {59}. Therefore, the metadacite and metarhylite probably reflect a mantle source with mainly amphibole and little or no clinopyroxene fractionation. On the other hand, the younger two-mica granites have an almost constant Zr/Y ratio with increasing Zr content, indicating fractionation of minerals to which both elements are equally incompatible. The major fractionating mineral of the two-mica granite is plagioclase, which is also responsible for the deep negative Eu anomalies (Fig. 3).

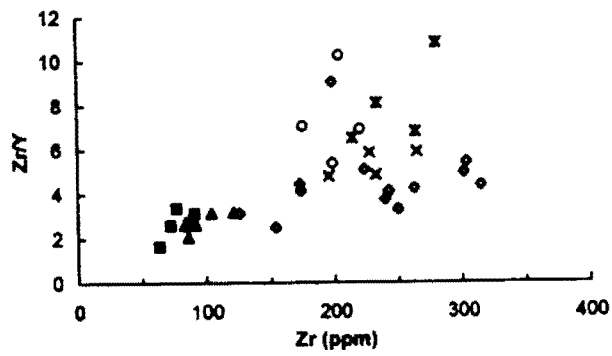

Figure 11: Zr. vs. Zr/Y diagram for the ophiolitic metagabbro & metabasalt, non-opiolitic metavolcanics and younger two-mica granite of the Zabara district. Symbols as in Figure 2.

REE modelling

Selection of mantle source (s) composition for the petrogenetic modelling is mainly based on the REE patterns of the different rock types in the Zabara district. The OMGB have REE patterns similar to N-MORB. These rocks could have been generated by different degrees of partial melting from an anhydrous spinel lherzolite source {81}.

The choice of REE concentration twice chondritic abundances for the mantle models has been assumed by {82, 83, 84}. The melting models used are those of {83}, who dealt with possible mantle sources for tholeiitic and calc-alkaline magmas in the Sunda arc (Indonesia). For all melting models the non-modal batch partial melting equation of {85} was applied.

OMGB: The average REE contents of the ophiolitic metagabbro and metabasalt was used in the modelling. The average REE pattern of the ophiolitic metagabbro can be modelled by a high degree (25 %) of no-modal batch partial melting of spinel lherzolite source (Ol_{58}, Opz_{20}, Opx_{20}, Sp_2 Modal %) and followed by subsequent 15 % fractional crystallisation of livine, clinopyroxene and plagioclase in proportions of 0.3, 0.45 and 0.25, respectively. The modelled primary melt has a REE pattern closely similar to the observed average pattern of the ophiolitic metagabbro (Fig.12A). On the other hand, the ophiolitic metabasalt could be generated by a lower degree (10 %) of batch partial melting of the same source (spinel lherzolite) followed by higher degree of fractional crystallization (25 %) mainly of olivine, clinopyroxene and plagioclase in the respective proportions 0.2, 0.4 and 0.4 (Fig. 12B). The modelling reveals the more dominant role of plagioclase removal during the evolution of the metabasalts as compared to the metagabbros. This is confirmed by the slight negative Eu anomalies in the metabasalt patterns, whereas those of the metagabbros have no Eu anomalies.

Non-ophiolitic metavolcanics: The nearly consistency of incompatible trace element ratios for the non-ophiolitic metavolcanics (Meta-andesites, metadacites and metarhyolites) such as Zr/Y (5.3, 8 and 7.4, respectively) and the similarities in the REE patterns (Fig. 3) suggests that these rocks are cogenetic. The REE patterns of the

non-ophiolitic metavolcanics are characterized by strong LREE-enrichment and relatively unfractionated, flat HREE. These patterns could no be produced by partial melting of a garnet-bearing mantle peridotite source, but rather may be generated by partial melting and fractional cystallisation of a hydrous lherzolite source (Ol_{60}, Cpx_{15}, Opx_{20} and $Amph_5$ modal %).

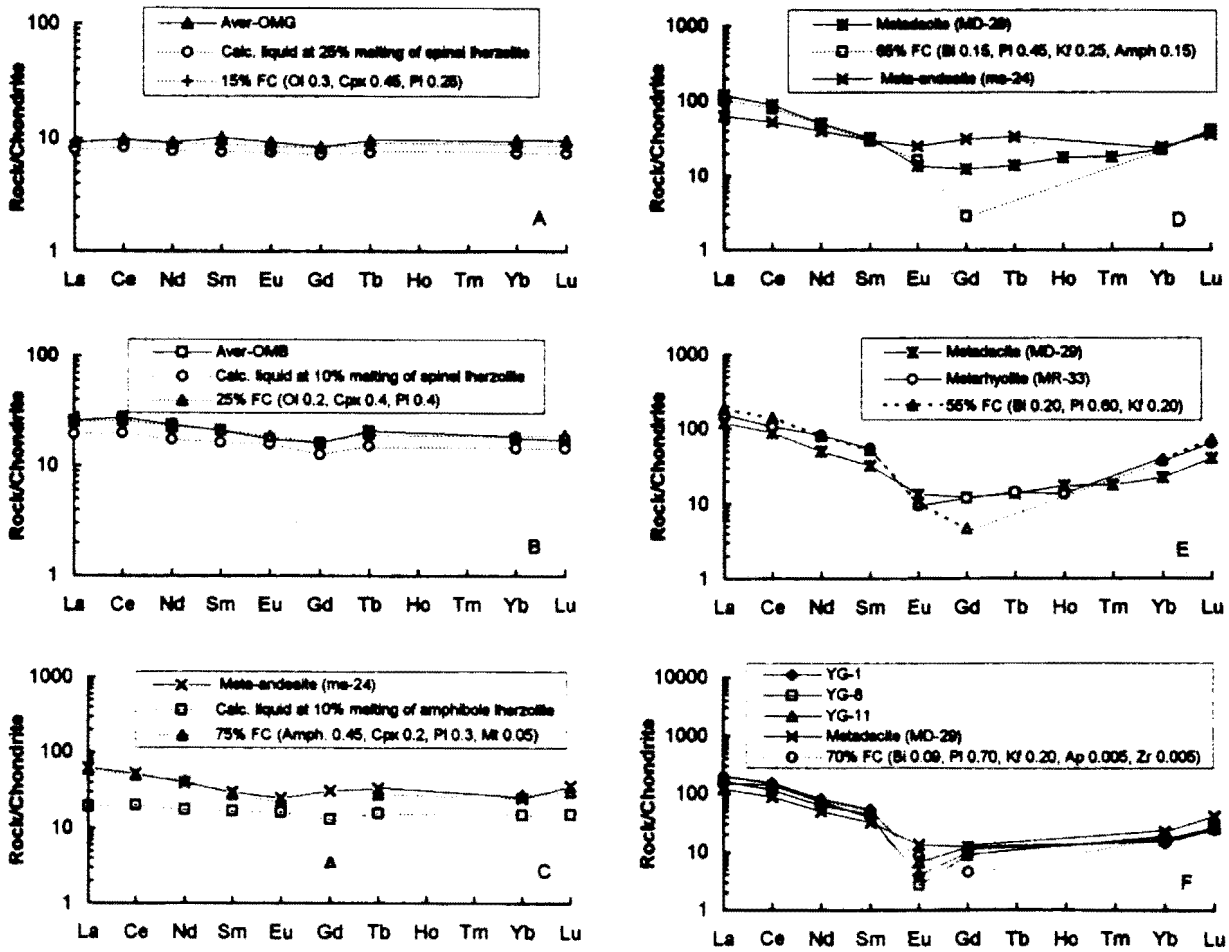

Figure 12: Rare earth elements (REEs) geochemical modelling for the ophiolitic metagabros (A), ophiolitic metabasalts (B), meta-andesites (C), metadacites (D), metarhyolites (E) and younger two-mica granites (F). Bi = biotite, Cpx = clinopyroxene, Pl = plagiocase, Mt= maganite, Kf = K- feldspar , Amph = amphibole, Ap = apatite and Zr = zircon. Partition coeficients are from different sources.

Depending on the REE patterns, the meta-andesites could be derived by 10% batch partial melting of an amphibole lherzolite mantle source followed by 75 % fractional crystallization of amphibole, clinopyroxene, plagioclase and magnetite in proportions of 0.45, 0.20, 0.30 and 0.05, respectively (Fig. 12C). Subsequently, the metadacites could be modelled by fractional cystallisation of the decived andesitic liquid. Figure 12D shows that the metadacite could be generated from the andesitic melt by about 65 % fractional crystallization of plagioclase, alkali feldspar, biotite and amphibole in proporotions of 0.45, 0.25, 0.15 and 0.15, respectively. Later, a fractional crystallization (55 %) dominantly of biotite, plagioclase and alkali feldspar (0.20, 0.60 and 0.20, respectively) from the evolved dacitic magma could yield a highly evolved rhyolitic liquid with a REE pattern similar to that observed for the metarhyolites (Fig. 12E). However, the modelled liquids have lower Gd contents than the investigated non-ophiolitic metavolcanics (Fig.12C, D and E).

Younger two-mica granites: these granites can be modelled by fractional crystallization (70 %) of plagioclase, alkali feldspar, biotite, titanite and zircon (0.70, 0.20, 0.90, 0.005 and 0.005, respectively) from the dacite magma (Fig. 12F). However, the investigated granites have higher Gd contents (3.32 ppm) than the modelled liquid (1.45 ppm).

CONCLUSIONS

The metamorphic rocks of the Zabara district composed of metasediments, an ophiolitic assemplage (serpentinites, metagabbros and metabasalts),non-ophiolitic metavolcanics ranging from meta-andesite to metarhyolite and younger two-mica granites. The major and trace elements of the metasediments are similar to the composition of the non-ophiolitic metadacites and metarhyolites. This feature suggests that the source rocks of the metasediments were similar in character to the non-ophiolitic metadacites and metarhyolites. The metasediments have immobile element contents closely comparable to ocean island arc metasediments.

The ophiolitic metagabbro and metabasalt display tholeiitic affinity and are similar to N-MORB. Geochemically, the ophiolitic rocks were generated by different degree of non-modal batch partial melting of spinel lherzolite source (25% for the metagabbro and 15% for the metabasalt) followed by fractional crystallization (15% for the metagabbro and 25% for the metabasalt) of livine, clinopyroxene and plagioclase. On the other hand, the well defined geochemical trends displayed by the non-ophiolitic metavolcanics suggest that the fractional crystallization has played a major role in their genesis. The meta-andesites can be modelled by 10% batch patial melting of amphibole lherzolite followed by fractional crystallisation of amphibole, clinopyroxene, plagioclase and magnetite. The metadacites can be produced by 65% fractional crystallization of the andesitic magma while the metarhyolite can be generated by about 55% fractional crystallisation of the dacitic magma. The younger two-mica granites, on the other hand, can be modelled by about 70% fractional crystallization of the dacitic magma.

ACKNOWLEDGEMENT

I Thank Dr. F.H. Mohamed for his assistance during the chemical analyses and for reading and earlier version of this work. I have benefitted from much useful discussions with Profs. S.O. Khalil and Y.M. Anwar. I am grateful to Dr. M.A. Obeid for his help during field work, and anonymous reviewer for constractive criticism.

REFERENCES

(1) Kroner, A. 1985. Ophiolites and the evolution of tectonic boudaries in the Proterozoic Arabian - Nubian Shield of Northeast Africa and Arabia. Precambrian Res., 27:277-300.

(2) Stoeser, D.E. and V.E. Camp, 1985. Pan-African microplate accretion of the Arabian Shield. Geol Soc. Amer. Bull., 96: 817-826.

(3) Pallister, J.S., J.S. Stacy, L.B. Fischer and W.R. Permo, 1988. Precambrian ophiolites of Arabia: geologic setting, U-Pb geochronology, Pb isotope characteristics and application for continental accretion. Precambrian Res., 38: 1-54.

(4) Gass, I.G. 1977, Evolution of the Pan-African crystalline basement in northeast Africa and Arabia J. Geol. Soc., London, 134: 129-138.

(5) El Ramly, M.F. 1972. A new Geological map for the basement rocks in Estern and Southwestern Desert of Egypt, scale 1: 1000000. Geol. Surv. Egypt, 2: 1-18.

(6) Vail, J.R. 1985. Pan-African (Late Precambrian) tectonic terrains and the reconstruction of the Arabian-Nubian Shield. Geology 13: 839-842.

(7) Bentor, Y.K. 1985. The crustal evolution of the Arabian -Nubian massif with special reference to the Sinai Peninsula. Precambrian Res., 28: 1-74.

(8) Stern, R.J. 1981. Petrogenesis and tectonic setting of late Precambrian ensimatic volcanic rocks, Central Eastern Desert of Egypt. Precambrian Res., 16: 195-230.

(9) El-Gaby, S., O.M. El Nady, and A.M. Kudier, 1984. Tectonic evolution of basement complex in the central Esatern Desert of Egypt. Geol. Rund., 73: 1019-1036.

(10) Akaad, M.K. and A.M. Noweir, 1980. Geology and lithostratigraphy of the Arabian Desert oro genic belt of Egypt between lat.25° 35° and 26° 30°. Institute of Application and Geology, Jeddah 3:127-134.

(11) El-Sharkawy, M.A. and R.M. El Bayoumi, 1979. The ophiolites of Wadi Ghadir area, Eastern Desert, Egypt. Geol. Surv. Egypt, 9:88-101.

(12) Shackleton, R.M., A.C. Ries, R.H. Garaham and W.R. Fitches, 1980. Late Precambrian ophiolit ic melange in the Eastern Desert of Egypt. Nature 285:472-474.

(13) Takla, M.A., M.A. El Sharkawy and F.F. Basta, 1982. Petrology of the basement rocks of Gabel Mohagara-Ghadir area, Eastern Desert, Egypt. Geol. Suv. Egypt, 12: 121-140.

(14) Stern, R.J. and C.E. Hedge, 1985 Grochronologic and isotopic constrainsts on Late Precambrian crustal evolution in the Eastern Desert of Egypt. Amer. J. Sci., 285: 97-127.

(15) El-Gaby, S., F. K. List, and R. Tehrani, 1988. Geology, evolution and metallogenesis of the Pan-African Belt in Egypt. In: El Gaby, S. and R. D. Greilling (eds.) The Pan-African Belt of The North East Africa and Adjacent Area. Vieweg, Eiesbaden.

(16) Kroner, A., W. Todt, I.M. Hussain, M, Mansour and A.A. Rashwan, 1992. Dating of Late Proterozoic ophiolites in Egypet and the Sudan using the single grain zircon evporation technique. Precam brian Res., 59:15-32.

(17) Ashmawy, M.H. 1987. The Ophiolitic mealange of the south Eastern Desert of Egypt: Remote sensing, Field work and petrographic investigation. Berlin Geowiss. Abhandl, 84 (A): 1-135.

(18) El-Gaby, S., F.K. List and R. Tehrani, 1990. The basement complex of the Eastern Desert and Sinai. In: R Said (ed) The Geology of Egypt. Balkeme Rotterdam, Netherlands, pp. 175-184.

(19) Basta, E. Z and M.A. Takla, 1974. Distribution of opaque minerals and the origin of the gabbroic rocks of Egypt. Fac. Sci. Bull. Cairo Univ, 47:347-364.

(20) Hassan, M. A. and A. H. Hashad, 1990. Precambrian of Egypt. In: R. Said (ed) The Geology of Egypt. Balkema rotterdam,Netherlands, pp. 201-248.

(21) Mohamed, F.H and M.A.Hassanen,1996. Geochemical evolution of arc-related mafic plutonism in the Umm Naggat district, Eastern Desert of Egypt. J. African Earth Sci., 22:269-283.

(22). Abdel-Rahman, A.M. 1996. Pan-African volcanism: petrology and geochemistry of the Dokhan Volcanic Suite in the northern Nubian Shield. Geol. Mag., 133: 17-31.

(23) Hashad, A.H. 1980. Present status of geochonological data on the Egyptian basement complex. Institut of Application Geology. Jeddah, 3: 31-46.(24) Sabet, A.H.

(24) 1972 . On the stratigraphy of the basement rocks of Egypt. Geol. Surv. Egypt 2:79-102.

(25) El Sayed, M.M. 1998. Tectonic setting and petrogenesis of the Kadabora pluton: A late protero zoic anorogenic A-type younger granitoid in the Egyption Shield. Chemie der Erde, 58: 38-63.

(26) Hussain, A.A. M.M. Ali, and M.F. El-Ramly, 1982. A proposed new Classification of the granites of Egypt. J. Volcan. Geother. Res., 14: 187-198.

(27) Jackson. N.J.N. Walsh and E. Pegram, 1984. Geology, geochemistry and petrogenesis of late Precambrian granitoids in the central Hijaz region of the Arabian Shield. Contrib. Mineral. Petrol., 87: 205-219.

(28) Klemenic, P. M. and S. Poole, 1988. The geology and geochemistry of Upper Proterozoic granitoids from the Red Sea hills, Sudan. J. Geol. Soc., London, 145: 635-643.

(29) Abu El Ela, F. F. and M. a. Hassan, 1992. Geology and geochemistry of bimodal volcanism north of Gabal Zabara, Eastern Desert, Egypt. Egypt. Jour. Geol. 36: 253-271.

(30) Berhe, S. M. 1990. Ophiolites in northeast and east Africa: implications for Proterozoic crustal growth. J. Geol. Soc., London, 147: 41-57.

(31) Cann, J.R. 1969. Spilites from the Carlsberg Ridge, Indian Ocean. J. Petrol., 10: 1-19.

(32) Hart, R.A. 19970. Chemical exchange between sea water and deep ocean basalts. Earth Planet. Sci. Letters, 9: 269-279.

(33) Melson, W. G. 1973. Basaltic glasses from the Deep Sea Drilling Project. Chemical characteristics, composition of alteration products, and fission track "ages". Trans. amer. Geophys. Union, 54: 1011-1014.

(34) Shido, F., a. Miyashiro and M. Ewig, 1974. Compositional variations in pillow lavas from the Mid-Atlantic Ridge. Marine Geol., 16:177-190.

(35) Zielinski, R.a. 1982. The mobility of uranium and other elements during alteration of rhyolite ash to montmorillonite: a case study in the Troublesome Formation, Colorado, U.S.A. Chem. Geol., 35:185-204.

(36) Hart, S. R., a. J Erland and E. J. K. kable, 1974. Sea floor basalt alteration: some chemical and Sr isotope effects. Contrib. Mineral. Petrol., 44:219-230.

(37) Humphris, s.e. and G. Thompson, 1978. Trace elements mobility during hydrothermal alteration of oceanic basalts. Geochem. Cosmoch. Acta, 42: 219-230.

(38) Pearce, J. A. 1987. An expert system for the tectonic characterization of ancient volcanic rocks. J. Volcan. Geother. Res., 32:51-65.

(39) Saunders, A. D., J. Tarnery and S. d. Weaver, 1980. Transverse geochemical variations across the Antarctic Peninsula: implications for the genesis of calc-alkaline magmas. Erth planet. Sci. Letters, 46:344-360.

(40) Wood, D. A., J. L. Joron and M. Treuil, 1979. A re-appraisal of the use of trace elements to classify and dicriminate between magma series erupted in different tectonic settings. Earth Planet. Sci. Letters, 45: 326-336.

(41) Pearce, J. a. 1975. Basalt geochemistry used to investigate past tectonic environments on Cyprus. Tectonophysics 25: 41-67.

(42) Shervais, J.W. 1982. Ti-V Plots and the petrogenesis of modern and ophiolitic lavas. Earth Planet. Sci. Letters, 59: 101-118.

(43) Furnes, H. 1978. Element mobility during palagonitization of a subglacial hyaloclastite in Iceland. Chem. Geol., 22:249-264.

(44) Furnes, H. 1980. Chemical changes during palagonitization of an alkaline olivine basaltic hyaloclastite, Santa Maria, Azores. Nees Jahrb. Mineral. abh., 138: 14-30.

(45) Staudigel, H. and S.R. Hart, 1983. alteration of basaltic glass: mechanism and significance for the oceanic crust-seawater budget. Geochim. Cosmochim. Acta, 47: 37-50.

(46) Mullen, E. D. 1983. MnO/TiO2/P2O5: a minor element discriminant for basaltic rocks of oceanic environments and its implications for petrogenesis. Earth Planet. Sci. Letters, 62:53-62.

(47) Merriman, R.J.R.E. Bevins and T.K. Ball, 1986. Petrological and geological variations within the Taly Fan intrusion: a study of element mobility during low grade metamorphism with implications for petrogenetic modelling. J. Petrol. 27:1409-1436.

(48) Blatt, H.G. Middlecton and R. Murray, 1980 Origin of Sedimentary Rocks. Pentice-Hall, Englewood Cliffs, New Jersey, 782 pp.

(49) Pettijohn, F.J., P.E. Potter and R. Siever, 1973. Sand and Sandstones. Springer-Verlag, New York, 618 pp.

(50) Roser, B.P. and R.J. Korsch, 1986. Determination of tectonic setting of sandstone-mudstone suites using SiO_2 content and K_2O/Na_2O ratio. J. Geol., 94: 635-650.

(51) Bhatia, M.R. 1983. Plate tectonics and geochemical composition of sandstones. J. Geol., 91: 611-627.

(52) Holland, H.D. 1978. The chemistry of the atmosphere and oceans. Wiley, New York, 351 pp.

(53) McLennan, S.M.S.R. Taylor and K.A. Eriksson, 1983. Geochemistry of Archean shales from the Pilbara Supergroup, Western Australia Geochim Cosmochim. Acta, 74: 1211-1222.

(54) Floyd, P.A. and J.A. Winchester, 1975. Magma type and tectonic setting discrimination using immobile elements. Earth Planet. Sci. Letters, 27: 211-218.

(55) Miyashiro, A. 1975. Classification, characteristics and origin of ophiolites. J. Geol., 83: 249-281.

(56) Gelinas, L., P. Trudel and C. Hubert, 1984. Chimico-stratigraphie du groupe de Blake River. Ministere del' Energie et des Ressources du Quebec, MM: 83-101.

(57) Pearce, J.A. and J.R. Cann, 1973. Tectonic setting of basic volcanic rocks determined using trace element analyses. Earth Planet, Sci. Letters, 19: 290-300.

(58) Pearce, J.A. 1976. Statistical analysis of major element patterns in basalts. J. Petrol., 17: 15-43.

(59) Pearce, J. A. and M.J. Norry, 1979. Petrogenetic implication of Ti, Zr, Y, and Nb variation in volcanic rocks. Contrib. Mineral. Petrol., 69: 33-47.

(60) Wood. D.A. 1980. The application of Th-Hf-Ta diagram to problems of tectonomagmatic classification and to establishing the nature of crustal contamination of basaltic levas of the British Tertiary volcanic province. Earth Plane. Sci. Letters, 50: 11-30.

(61) Meschede, M. 1986. A methode of discriminating between different types of mid-ocean ridge basalts and continental tholeiites with the Nb-Zr-Y diagram. Chem. Geol., 56: 207-216.

(62) Peccerillo, A. and S.R. Taylor, 1976. Geochemistry of Eocene calc-alkaline volcanic rocks from the Kastamonu area, northern Turkey. Contrib. Mineral. Petrol., 58: 63-81.

(63) Tatsumi, Y. 1990. Geochemical evolution of the mantle wedge. In: F. Marumo (ed) Dynamc Processses of Material Transport and Transformation in the Earth's Inerior. Terra Scientific , Tokyo, pp. 313-345.

(64) Pearce, J.A., N.B. Harris and A.G. Tindle, 1984. Trace element discrimination diagrams for the tectonic interpretation of granitic rocks. J. Petrol., 25: 956-983.

(65) Liegeois, J.P. and R. Black, 1987. Alkaline magmatism subsequent to collision in the Pan-African belt of the Adrar des lforas (Mali). In: JG Fitton, BJG Upton (eds). Alkaline lgneous Rocks. J. Geol. Soc., Spec. Publ., 30: 381-401.

(66) Dewitt, E. 1989. Geochemistry and tectonic polarity of Early Proterozoic (1700-1750 Ma) plutonic rocks, north-central Arizona Goel. Surv. Deigest., 17: 149-164.

(67) Clark, D.B. 1981. The mineralogy of peraluminous granites: a review. Canad. Mineral., 19: 3-17.

(68) Debon, F. and P. Le Fort, 1983. A chemical-mineralogical classification of common plutonic rocks and association. Trans. Roual Soc. Edinburgh Earth Sci., 73: 135-149.

(69) Debon, F. and P. Le fort, 1988. A cationic classification of common plutonic rocks and their magmatic associations. Pincipales, methods, applications. Bull. Mineral., 111: 493-510.

(70) Whalen, J. B., K.L. Currie and B. W. Chappel, 1987. A-type granites: geochemical charactyeristics, discrimination and petrogenesis. Contrib. Mineral. Petrol., 95: 407-419.

(71) Eby, G.N. 1990. The A-type granitoids: A review of their occurrence and chemical characteristics and speculations on their petrogenesis. Lithos 26: 115-134.

(72) Eby, G.N. 1992. Chemical subdivision of the A-type granitoids: petrogenetic and tectonic implications. Geollogy 20:641-644.

(73) Anderson, J.L. and r.L. Cullers, 1978. Geochemistry and evolution of the Rolf River Batholith, a late precambrian rapakivi massif in north Wisconsin, U.S.A. Precambrian Res., 7: 287-324.

(74) Misra, K.C. and J. A. Conti, 1991. Amphibolites of the Ashe and Alligator Back Formations, North Carolina: samples of late Proterozoic-early Paleozoic oceanic crust. Geol. Soc. Amer. Bull., 103: 737-750.

(75) Wilson, M. 1989. Igneous petrogenesis - A Global Tectonic Approch Unwin Hyman. London Boston Sydney Wellington. 466 pp.

(76) Perfit, M.R., D.A. Fust, E. Bence, R. J. Arculus and

S.R. Taylor 1980. Chemical characteristics of island arc basalts: implication for mantle source. Chem> Goel., 30: 256-277.

(77) Hanson, G. N. 1978. The application of trace elements to the petrogenesis of igneous rocks of graitic composition. Earth Planet. Sci. Letters, 38: 26-43.

(78) Pearce J A (1980) Geochemical evidence for the genesis and eruptive setting of levas from Tethyan ophiolites. Proc. Inter. Ophiolite Symposium, Nicosia, Cyprus, 261-272.

(79) Rajamani v., K. Shivkumar. G,N. Hanson and S.B. Shirey, 1985. Geochemistry and petrogenesis of amphibolites, Kolar Schist Belt, south India: evidence for komatiitic magma derived by low percentages of melting of the mantle. J. Petrol., 26: 99-123.

(80) Hart, S. R. and T. Dunn, 1993. Experimental cpx/melt partitioning of 24 trace elements Contrib. Mineral. Petrol., 113: 1-8.

(81) Takahashi, E. and I. Kushiro, 1983. Melting of a dry peridotite at high pressures and basalt magma genesis. Amer. Mineral., 68: 859-879.

(82) Haskin, L., M.A. Haskin, F. A. Frey and T.R. Wildeman, 1968. Relative and absolute terrestrial abundances of the rare earths. In; L.H. Ahrens (ed) Origin and distribution of the elements. Pergamon Press, New York, pp. 889-912.

(83) Nicholls, I. A., D. J. Whitford, K. L. Harris and S.R. Taylor, 1980. Variation in the geochemistry of mantle sources for tholentic and calc-alkaline mafic magmas, western sunda volcanic arc, Indonesia. Chemi. Geol., 30: 177-199.

(84) Thompson, R.N., M.A. Morrison, G.L. Hendry and S.J. Parry, 1984. An assessment of the relative roles of crust and mantle in magma genesis: an elemental approach. Philosl. Trans. Royal Soc. London, A310: 549-590.

(85) Shaw, S.M. 1970. Trace element fractionation during anatexis. Geochim. Consmochim. Acta, 34: 237-243.

(86) Bhatia, M.R. and K.A.W. Crook, 1986. Trace element characteristics of greywackes and tectonic setting discrimination of sedimentary basins. Contrib. Mineral. Petrol., 92: 181-193.

(87) Pearce, J.A. 1982. Trace element characteristics of lavas from destructive plate boundaries. In: R.S. Thorpe, (ed) andesites, Orogenic andesites and related rocks. Wiley and Sons, Chichester, pp. 525-548.

(88) Streckeisen, A. and R.W. Le Maitre, 1979. A chemical approximation to the modal QAPF classification of the igneous rocks. Neues Jahrb. Mineral. Abhefte, 136: 169-206.